JOURNAL OF CHEMICAL INFORMATION AND MODELING

Article

pubs.acs.org/jcim

Experimental-Like Affinity Constants and Enantioselectivity Estimates from Flexible Docking

N. J. Gumede,[†,‡] P. Singh,[‡] M. I. Sabela,[‡] K. Bisetty,[‡] L. Escuder-Gilabert,[§] M. J. Medina-Hernández,[§] and S. Sagrado*[,§,∥]

[†]Department of Chemistry, Mangosuthu University of Technology, P.O. Box 12363, Jacobs, 4026, South Africa

[‡]Department of Chemistry, Durban University of Technology, P.O. Box 1334, Durban, 4000, South Africa

[§]Departamento de Química Analítica, Facultad de Farmacia, Universidad de Valencia, Burjassot, Valencia, Spain

[∥]Centro de Reconocimiento Molecular y Desarrollo Tecnológico (IDM), Unidad mixta Universidad Politécnica de Valencia−Universidad de Valencia, Valencia, Spain

ABSTRACT: Experimental-like affinity constants and enantioselectivity estimates, not predicted so far computationally, were obtained using a novel flexible modeling/docking combined strategy. The *S*- and *R*-warfarin−human serum albumin (HSA, site I) complexes were used as an interaction model. The process for a verified estimation includes the following: (i) ionized open chain forming at physiological pH (a recent focus); (ii) conformational search (molecular mechanics and Monte Carlo methods); (iii) rigid protein−flexible ligand docking (GlideXP) generating low energy paired *S*- and *R*-poses; (iv) graphical comparison against the X-ray crystal structure (unsatisfactory verification step); (v) quantum polarized ligand docking (insufficient verification step); (vi) induced fit docking (one pose satisfying the verification criterion; selection step); (vii) converting docking scores to affinity and enantioselectivity estimates (log K_S = 5.43, log K_R = 5.34, ES = K_S/K_R = 1.23) and numerical comparison against equivalent literature data from bioanalytical techniques (validation step); (viii) intermolecular forces explaining ES (hydrogen bonding and $\pi-\pi$ interactions).

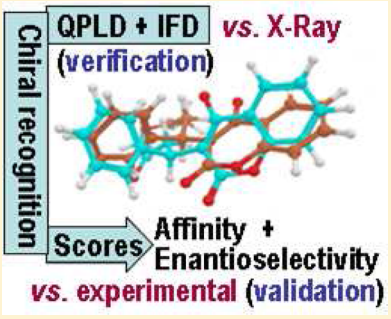

INTRODUCTION

Drug action in living organisms results from a series of pharmacological processes prior to reaching the target to elicit a pharmacological effect. Most of these processes present a higher degree of enantioselectivity resulting in differences between the activities of drug enantiomers. The key to improving their efficiency and efficacy is based on enantiomers that possess a major therapeutic effect (eutomers), thus eliminating those with no/minor therapeutic effect or providing side effects (distomers).[1,2] Among others, interactions with plasma proteins are decisive features characterizing the biological activity of therapeutic drugs.[3] Furthermore, enantioselectivity in protein binding can have a significant effect on the pharmacokinetics and pharmacodynamic properties of chiral therapeutics. Human serum albumin (HSA) has mainly attracted the pharmaceutical industry's attention because of its binding ability to a variety of drugs and exogenous compounds (promiscuity) with higher affinity. Moreover, it has the potential to exhibit the highest enantioselectivity among the plasmatic proteins.[4,5] In most cases, the focus of attention has been directed to high affinity HSA sites, i.e., site I (warfarin site) and site II (diazepam site); this is because the in vivo concentration of administered drugs is mostly lower than that of HSA by 600 μM.[6]

Bioanalytical methodologies have extensively been used to assess the drug−protein interactions, in terms of binding affinity quantification, and, more recently, enantioselectivity quantification. The most important analytical approaches to characterize drug−protein binding have been critically reviewed.[7] Also, microseparation techniques for evaluating the enantioselective binding of drugs to plasma proteins have been reviewed.[3] It is generally assumed that quantitative estimates from bioanalytical methods are accurate enough; however, the quality of the results is rarely verified, resulting in a risk of errors over published results.[8,9] Moreover, bioanalytical studies could not provide information related to the identification of molecular mechanisms involved in the affinity and enantiodiscrimination. Several relatively uniform experimental data on warfarin enantiomer−HSA affinity constants (and then enantioselectivity) are available in the literature.[10−14]

Computational prediction of protein affinity/enantioselectivity is of interest for avoiding the use of expensive and time-consuming experiments. However, molecular docking is still far from being considered a fully validated methodology and the binding affinity estimation is software/protocol dependent. Commercially available docking software programs provide docking scores as outputs based on scoring functions to approximate binding free energies,[15−17] which measure the binding affinity degree of the ligand to a protein.[18] They can be

Received: July 17, 2012

   dx.doi.org/10.1021/ci300335m | *J. Chem. Inf. Model.* XXXX, XXX, XXX−XXX

used to discriminate between binders and nonbinders of a given protein−ligand pose, in relation to the ability to fit snugly to the active site pocket depending on the steric clashes between the amino acid residues of the protein and the functional groups of the ligand. The correlation of docked scores with experimentally determined binding affinities has been a challenge for docking processes in recent years.[19] However, a direct estimation of experimental-like affinity constants and enantioselectivity would be necessary to facilitate the essential validation step of molecular modeling/docking estimates. Until now, the docking scores have not yet been converted directly into experimental-like parameters for direct comparison (e.g., validation) purposes.

Molecular docking approaches have a distinctive ability to reveal data at a molecular level as well as forces associated with affinity/enantioselectivity information. This task should be more realistic if previous experimental-like quantitative docking estimations have been validated. Several rules/improvements have been suggested in order to generate poses reflecting the real in vivo situation, e.g., poses that can be superimposed onto X-ray crystal structures.[20] It has been stated that in most cases incorrect sampling of partial charges of atoms provides inadequate poses, which can be solved by using quantum mechanical/molecular mechanics (QM/MM) approaches. It has been reported that rigid receptor docking approaches can succumb to incorrect poses in the case of flexible proteins, caused by conformational changes within the receptor and the ligand during the binding event.[21,22] In the case of warfarin enantiomers interacting with HSA, Bos et al.[22] indicated a two-step binding process where the ligand binds to HSA rigidly in the first step, while HSA undergoes slow conformational changes to accommodate them in the second step where the ligand−protein complex is formed. In this sense, Schrödinger's quantum polarized ligand docking (QPLD)[23] and induced fit docking (IFD)[24] modules have been developed to improve sampling of partial charges and side-chain and backbone movements of the protein, respectively.

Warfarin is a typical HSA site I marker. To the best of our knowledge, only one computational study on the racemic warfarin−HSA interaction has been reported.[19] No computational study has been performed on the chiral recognition of this interaction. The aim of this work is to optimize a combined molecular modeling/docking approach to cover two objectives: (i) reliable quantitative estimation of experimental-like affinity/enantioselectivity parameters (able to be directly compared with available equivalent in vivo/in vitro data) and (ii) reliable identification of molecular mechanisms involved in the obtained affinity/enantioselectivity (chiral recognition). A novel combination of commercially available programs, which includes Schrödinger's QPLD and IFD modules, together with a verification step, based on the comparison of docking poses obtained against the X-ray crystal strucuture (*R*-warfarin−HSA site I complex), is proposed, as a relatively simple and inexpensive computational tool ready to complement experimental approaches.

MATERIALS AND METHODS

Software. All computational studies were carried out using a series of modules in the Schrödinger 2011 suite with Maestro 9.2,[25] which is a graphical user interface such as Glide 5.7[26] and Macro Model 9.9,[27] to mention just a few.

Protein Selection and Preparation. The three-dimensional (3D) crystallographic HSA structure was obtained from the RCSB Protein Data Bank (PDB). Specifically, the crystal structure of HSA cocrystallized with *R*-warfarin in the active site I (PDB code 2BXD; subdomain IIA), with a resolution of 3.05 Å, was selected. The downloaded structure was subjected to Maestro's protein preparation module.[28] The following steps were accomplished: (i) Hydrogen atoms were added to the crystal structure. (ii) The side-chain residues of glycine and aspartic acid were allowed to rotate in order to maximize hydrogen bond interactions. (iii) Schrödinger's Prime 3.0 module[29] was used to fill in the missing side chains. (iv) Water molecules within 5 Å of the cocrystallized ligand were removed. (v) The pH of the entire system was adjusted to 7.4 using Epik.[30] (vi) The hydrogen bonding network was optimized, and finally a geometry optimization was performed to a maximum root-mean-square deviation (rmsd) of 0.30 Å using the OPLS_2005 force field.

Ligand Preparation and Conformational Search. Schrödinger's Ligprep 2.5[31] was used to generate 3D structures of ligands maintaining the stereochemistry encoded in the original file. For this purpose enantiomeric pairs for warfarin were generated. Additionally, the ionization states for the tautomeric forms of warfarin were predicted using Schrödinger's Epik[30] module at pH 7.4 (ionization constant pK_a = 5.1 for warfarin enantiomers was predicted). The extensive conformational search was performed using the Monte Carlo Multiple Minimum (MCMM) search algorithm implemented in Schrödinger's MacroModel 9.9 program coupled with the OPLS_2005 force field under implicit solvent conditions using the GB/SA approximation. Thereafter, the ligands were subjected to a series of energy minimization steps, using the MM minimization with the PRCG (Polak−Ribiere-type conjugate gradient) method.

Glide XP Procedure. Schrödinger's docking algorithm implemented as Glide (grid based ligand docking with energetics) was used to predict the binding affinities and binding geometries for the HSA−ligand complexes, marking the hydrogen bond and the position of the ligand in the active site I. Initial docking calculations were performed in extra precision mode using GlideXP[26] with standard van der Waals scaling of 0.8 to include modest "induced fit" effects. The two conformers with the lowest estimated potential energy were selected for further calculations (next procedures).

Quantum Polarized Ligand Docking (QPLD) Procedure. The two selected conformers from GlideXP were used as starting geometries for the QM-Polarized Ligand Docking approach, QPLD[23,32] (a recent ab initio methodology from Schrödinger to calculate ligand charges within the protein environment). The first step involves the generation of quantum mechanical charges for the free ligand performed at the density functional theory (DFT) level using the B3LYP functional and the 6-31G* basis set within the Jaguar module.[33] The protein was subsequently modeled with the MM methods using the OPLS_2005 force field. Ligands were redocked using GlideXP included in QPLD to generate poses.

Induced Fit Docking (IFD) Procedure (QPLD + IFD Approach). The two QPLD conformers were submitted as starting geometries to IFD[24] calculations using Glide 5.7.[26] In the first IFD stage, a softened-potential docking was performed using GlideSP (Standard Precision) mode generating 20 initial poses. For each one, a full circle of protein refinement was performed using Prime 3.0.[29] Residues of the protein within 5.0 Å of ligand poses were refined, and side chains were conformationally changed and subsequently minimized.

dx.doi.org/10.1021/ci300335m | J. Chem. Inf. Model. XXXX, XXX, XXX−XXX

Table 1. Experimental[a] and Computational[b] Affinity Constants (in Logarithmic Form) and Enantioselectivity (ES = K_S/K_R)

ID (ref, year)	details	log K_S	log K_R	ES
1[a] (10, 1971)	equilibrium dialysis (in solution); pH 10	5.39	5.31	1.18
2[a] (11, 1977)	equilibrium dialysis (in solution)	5.76	5.40	2.28
3[a] (12, 1983)	immobilized HSA; zonal elution; buffer concentration 0.04 M	5.64	5.52	1.33
4[a] (13, 1994)	immobilized HSA; frontal analysis	5.41	5.32	1.24
5[a] ([14], 1998)	equilibrium dialysis (in solution)	5.29	5.01	1.92
6[b] (this work)	conformers ranked by potential energy; showing results of paired *S*-and *R*-poses from two conformers with lowest potential energy	4.47	3.89	3.86
		4.53	4.49	1.10
7[b] (this work)	conformers in ID6 submitted to QPLD as intermediate approach; showing results of corresponding paired *S*-and *R*-poses	4.87	4.86	1.01
		4.85	4.84	1.03
8[b] (this work)	conformers in ID7 submitted to IFD as intermediate approach; showing results of paired *S*-and *R*-poses satisfying verification criteria[c]	5.43	5.34	1.23

[a]All experimental data correspond to equilibrium approaches at pH 7.4 (0.067 M phosphate buffer) and 37 °C (except when indicated). [b]A sequential cumulative protocol is used (ID 6, then ID 7, and finally ID 8). [c]The predicted *R*-pose should superimpose to the X-ray crystal structure (2BXD).

Ligands were redocked with GlideXP included in IFD to generate poses.

Outputs' Transformation To Obtain Final Useful Parameters. Docking scores from GlideXP (in kcal mol^{-1}) were understood as standard Gibbs free energy change, ΔG°[16,34−36] concretely as the apparent free energy change corresponding to near-physiological conditions[37−39] (for simplicity we keep the nomenclature ΔG°). In this work, these values were converted to affinity constants for both enantiomers, K_E (M^{-1}), based on the following equation:

$$K_E = e^{(-\Delta G^{\circ}_E/RT)} \quad (1)$$

where ΔG°_E is the apparent Gibbs free energy change for an enantiomer (in kcal mol^{-1}), R is the gas constant, 1.9872 × 10^{-3} (in kcal mol^{-1} K^{-1}), and T is the absolute temperature, here selected close to the physiological one, 310.15 (in K). From eq 1

$$\log K_E = -(\Delta G^{\circ}_E/2.3026RT) \quad (2)$$

$$ES = K_S/K_R = e^{[(\Delta G^{\circ}_R - \Delta G^{\circ}_S)/RT]} \quad (3)$$

RESULTS AND DISCUSSION

Affinity Data for Warfarin Obtained by Docking. Although computational quantitative affinity data for warfarin enantiomers (and therefore enantioselectivity data) are unavailable for comparison purposes, affinity data related to racemic warfarin have been reported.[19] The authors provided ΔG values ranging from −6.93 to −7.78 kcal mol^{-1}, corresponding to different molecular dynamics (MD) simulation times. Using their data in eq 2, we calculated the corresponding log K values ranging from 4.88 to 5.48. It should be noted that these results correspond to a quite different computational approach from the one proposed here.

Experimental Quantitative Affinity Constants and Enantioselectivity (ES) Data for Warfarin Obtained by Bioanalytical Techniques (Literature Data). Table 1 shows log K for each enantiomer and ES experimental results obtained from those bioanalytical approaches working in similar conditions, close to the physiological ones (ID 1−ID 5). Results indicate that the *S*-enantiomer has a moderately higher binding affinity to HSA than the *R* antipode (ES > 1). Combining the data in Table 1, reasonably good precision statistics on log K for enantiomers are encountered (relative standard deviation (RSD) ∼ 3.5%). In contrast, since ES comes from a ratio of affinity constants, imprecision becomes high (RSD > 30%). Robust statistics have been recommended in these studies.[8,9] Since the *median* from log K values corresponds to one of the paired data (ID 4), a reasonable averaged ES estimation can be the one corresponding to these values (ES = 1.24). This value, as well as the corresponding affinity constants (log K_S = 5.41 and log K_R = 5.32), can be used to further validate the computational estimation. Both results are consistent with the range computationally estimated for racemic warfarin.

Quantitative Binding Affinity/Enantioselectivity Estimations Using a Flexible Ligand−Rigid Receptor Approach (GlideXP). Both ionized and neutral forms of warfarin tautomers[29] (see Figure 1) were considered during ligand preparation to account for the broadest interaction possibilities. All forms were subjected to a conformational search algorithm, and the lowest energy conformers were subsequently subjected to the docking calculations. The results (not shown) indicated that anionic forms have lower energies than the neutral ones, as expected according to the fixed pH value and the pK_a of warfarin.

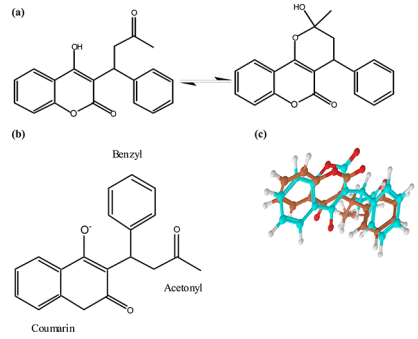

Figure 1. (a) Open chain (acyclic) tautomer (left) and close chain (cyclic hemiketal) tautomer (right) forms of neutral warfain. (b) Anionic open chain form of *S*-warfarin. (c) Selected *R*-warfarin pose (anionic open chain; ID 8 in Table 1) from IFD (brown), superimposed to *R*-warfarin enantiomer from 2BXD X-ray crystal structure (blue), indicative of a reasonable similarity in geometric arrangement of atoms in space. This was used as a verification criterion to decide on the acceptable docking solutions.

dx.doi.org/10.1021/ci300335m | J. Chem. Inf. Model. XXXX, XXX, XXX−XXX

Table 2. Molecular Docking Results at Molecular Level[a] for the Selected Pose Predicted by IFD (ID 8 in Table 1), with ES = 1.23, Similar to the Experimental One (ES = 1.24)

enantiomer	group (atom, rings)[b]	HSA residues (contacts)	H-bond distance (Å)	other electrostatic interactions	docking score (kcal mol^{-1})	K (M^{-1})
S	O$^-$ coumarin	Arg218 (N−H)	1.811			
	C=O coumarin	Tyr150 (O−H)	1.915			
	C=O acetonyl	Lys199 (N−H)	1.928			
	C=O coumarin	His242 (N−H)	2.190		−7.71	2.69 × 10^5
	coumarin	Tyr150 (Ar−H)	−	$\pi-\pi$		
	coumarin	His242 (Ar−H)	−	$\pi-\pi$		
R	C=O acetonyl	Lys199 (N−H)	1.868			
	O$^-$ coumarin	Arg257 (N−H)	1.877			
	O$^-$ coumarin	Arg257 (N−H)	2.033		−7.58	2.20 × 10^5
	O$^-$ coumarin	Tyr150 (O−H)	2.192			
	benzyl	His242 (Ar−H)	−	$\pi-\pi$		

[a]H-bonding (and its distance) and $\pi-\pi$ interactions are indicated as the main driving forces involved in enantioselectivity. Ar refers to an aromatic group of amino acids. Hydrophobic contacts were 122 029 and 122 107 kcal mol^{-1}, for *S*- and *R*-poses, respectively, suggesting that they do not define the enantioselectivity. [b]Figure 1a.

On the other hand, none of the *R*-poses found reproduced the structure of *R*-warfarin obtained from its crystal structure (PDB ID 2BXD), used as a verification step. Specifically, the *R*-poses revealed a noticeable change in the conformation of the rotatable groups in site I of HSA to accommodate the ligand. This occurs because only the rotatable groups of the amino acids in the binding site pocket are allowed to move freely and this movement changes the orientation of the ligand in the active site. Thus, the rigid receptor−flexible ligand approach employed, based on a lock and key approach (static event), seems to be incorrect in this case. In other words, the warfarin−HSA binding seems to be a dynamic event. This further suggests that HSA undergoes some induced fit effects and backbone movements when bound to the ligand, as previously reported.[18,21]

The two anionic open chain conformers exhibiting the lowest potential energy, thus representing the most stable paired *S*- and *R*-poses from GlideXP, were considered for further studies. Just for comparison purposes (these poses were considered unreliable to derive proper quantitative estimates), their corresponding docking scores were transformed into affinity/enantioselectivity estimates applying eqs 2 and 3 (ID 6, Table 1).

Quantitative Binding Affinity/Enantioselectivity Estimations Using a Quantum Polarized Ligand Docking (QPLD) as Intermediate Step. The selected conformers (ID 6, Table 1) were considered as initial structures and submitted to the intermediate QPLD step. Since they are anionic, probably the partial charges were not fully sampled during docking in the previous section. In most instances, the force field used in GlideXP does not accurately distribute formal ionic charges, and on top of that, it does not incorporate polarization effects,[18] which can be important in reproducing the poses with experimentally determined X-ray crystal structures. The hybrid QM/MM technique employed in QPLD has been suggested to overcome this limitation,[18,40] allowing an improved sampling of partial charges of the ligands prior to docking.[40−42]

As before, pairs of *S*- and *R*-poses were obtained. Compared with the poses in ID 6, the new generated *R*-poses showed improved geometric orientations with respect to the X-ray crystal structure. The benzyl and acetonyl groups were superimposable with the cocrystallized structure, but the coumarin ring showed an opposite conformation. Again, these poses were considered unreliable to derive suitable quantitative estimates.

As before, just to follow the evolution of the results, the scores from two pair of poses, selected according to the potential energies of the conformers, were again transformed into affinity/enantioselectivity estimates applying eqs 2 and 3 (ID 7, Table 1). An increase in log K values in ID 7 (with respect to ID 6) can be observed. The affinity (log $K \sim 4.8$) is now closer to those of the racemic warfarin and the experimental ones (Table 1), suggesting that sampling correction of atomic charges goes in the direction of improving the binding affinity estimations. The ligands and the receptor could be subjected to conformational changes during the binding process. Due to a rigid receptor approach employed (GlideXP) in the docking step, the receptor's flexibility is still sacrificed, thus generating poses that do not give a desirable reflection of the correct orientation of the poses. A way to compensate this could be the introduction of induced fit effects before the docking step.

Quantitative Binding Affinity/Enantioselectivity Estimations Using a Flexible Protein−Ligand/Induced Fit Docking (IFD) as Intermediate Step. The selected conformers (ID 7, Table 1) were considered as initial structures and submitted to the intermediate IFD step (then final outputs accumulate two treatments QPLD + IFD). IFD allows for the consideration of side chains and backbone movements of the protein when bound to the ligand molecule. As before, the resulting *R*-poses were graphically compared with the *R*-warfarin structure from the X-ray crystal structure. Only one *R*-pose was satisfactorily encountered and was considered the proper structure; note that an exact superimposition should not be expected.[43−45] The structures of the corresponding paired poses are shown in Figure 1.

Table 1 shows the quantitative results for the corresponding *S*- and *R*-poses (ID 8). The log K values in ID 8 are higher than those from the previous computational estimates, ID 6 and ID 7. Now, they are almost equal to the accepted reference experimental results (log K_S = 5.43 and log K_R = 5.34 in ID 8 versus log K_S = 5.41 and log K_R = 5.32 in ID 4). These results are also coherent with the computational estimated range for racemic warfarin (4.88−5.48). In terms of enantioselectivity, the comparison ID 8 (ES = 1.23) versus ID 4 (ES = 1.24) is again satisfactory (Table 1).

dx.doi.org/10.1021/ci300335m | J. Chem. Inf. Model. XXXX, XXX, XXX−XXX

Thus, the three combined quantitative experimental estimates (log K_S, log K_R, and ES) serve to validate the computational result, suggesting that the combined molecular modeling/docking approach (QPLD + IFD), guided by the graphical comparison with the crystal structure, as a verification/selection criterion, seems to be an applicable strategy for quantitative binding affinity/enantioselectivity estimations.

Molecular Level−Chiral Recognition Study. From previous sections, it can be assumed that the binding process of warfarin enantiomers to HSA involve changes in the conformation of the protein's active site I to accommodate the ligands, which should direct the subsequent change in the conformation of the ligands to adapt to its new host in the active site pocket. Also, they suggest that this process is affected by the chiral nature of the warfarin molecule. Table 2 shows the predicted molecular level interactions associated with the *S*- and *R*-poses in ID 8.

In previous work on racemic warfarin based on a different computational strategy,[19] the authors reported that the side chains Lys199, Arg257, and His242 were in direct contact with the ligand, although the nature of the interactions was not indicated as such. It can be noted that these three residues are present in the estimations made here for the *R*-pose, while two of them (Lys199 and His242) coincide with the *S*-pose (Table 2). Another report on the analysis of the experimental X-ray crystal structures for *R*-warfarin and *S*-warfarin enantiomers complexed with HSA[5] revealed the architecture of the two primary binding sites of HSA. In relation to site I, the authors report that Tyr150 assumes a central role for hydrogen bonding, followed by His242, Lys199, and Arg222. All, except Arg222, residues were encountered here as responsible for the hydrogen bonding of *S*-warfarin to HSA (Table 2). Furthermore, Petitpas et al.[45] pointed out that steric hindrance between Trp214, Arg218, and the benzyl ring of warfarin reduces the binding affinity of warfarin to HSA. Table 2 indicates the importance of Arg218−coumarin H-bond, only in the case of *S*-warfarin, which could compensate for the previously reported negative effect, justifying the higher affinity observed experimentally for this enantiomer.

On the other hand (Table 2, footnote [a]), hydrophobic contacts (slightly higher for the *R*-pose) are not consistent with the enantioselectivity observed, and it seems to contribute only to the high affinity predicted for the warfarin−HSA complex. A comparison of the results obtained for the *S*- and *R*-poses depicted in Table 2 suggests that two main interactions justify the enantioselectivity observed in favor of the *S*-pose: (i) its strong hydrogen bond (short distance) between the N−H group of Arg218 as a hydrogen bond donor and a negatively charged oxygen group of coumarin ring as a hydrogen bond acceptor, with a bond radii of 1.811 Å (Table 2), and (ii) its extra $\pi-\pi$ interaction.

CONCLUSIONS

A combined computational strategy (pose generation + graphical selection) allowed us to obtain optimized numerical docking outputs extrapolated into experimental-like affinity/enantioselectivity data, tested here for the unexplored chiral warfarin−HSA (site I) interaction. This includes a novel arrangement of the commercially available molecular modeling/docking approaches (QPLD + IFD) to provide the *S*- and *R*-poses (pose generation), but also a verification step, based on the *R*-warfarin structure (from the experimental X-ray crystal complex), which is used for the graphical inspection of the *R*-poses and the final selection of the accepted pair of *S*- and *R*-poses (graphical selection). The joint strategy should provide potentially improved practical results (here log K_S = 5.43, log K_R = 5.34, ES = K_S/K_R = 1.23). In the case of available alternative data (e.g., an averaged experimental data from bioanalytical techniques), the critical validation step is possible, thus serving to reinforce the reliability of the strategy. Moreover, the verified results are valuable to be compared with outputs from alternative computational strategies/protocols/commercial docking programs.

Novel aspects proposed, such as the generation of ionized tautomeric forms of enantiomers at physiological pH, which widens the range of potential for low energy conformers produced, should also be taken into account for future docking projects. The unsatisfactory verification against the X-ray crystal structure at this point suggests that the lowest energy anionic open chain warfarin enantiomers do not follow a "lock and key" approach when binding to the HSA site I pocket, i.e., a rigid protein−flexible ligand docking approach alone is unacceptable. This promotes successive intermediate modifications of the protocol in order to improve the results: here, for instance, incorporating the recent QPLD (to improve sampling of partial charges), hopeful but insufficient, and finally IFD (to improve the overall flexible interaction), to obtain a verified solution. In the future, newly developed computational alternatives could be tested in this way.

In addition, obtaining verified, and if possible, validated results allows extracting reasonably consistent information on the intermolecular forces involved in both affinity and enantioselectivity (independent) aspects. In this case, while mainly hydrophobic interactions probably help only in the high affinity observed, hydrogen bonds and $\pi-\pi$ interactions seem to define the moderate enantioselectivity in favor of *S*-warfarin, once mutual enantiomer−residue conformational changes, suggested by IFD, are produced.

AUTHOR INFORMATION

Corresponding Author

*E-mail: sagrado@uv.es. Fax: +34-963544953.

Notes

The authors declare no competing financial interest.

ACKNOWLEDGMENTS

The authors acknowledge the Universidad de Valencia, Project UV-INV-AE112-66280, for financial support. N.J.G. acknowledges the National Research Foundation, Project UID 80659, and the Research and Technology Transfer Directorate at Mangosuthu University of Technology, Project NSI/02/2010.

REFERENCES

(1) Chuang, V. T. G.; Otagiri, M. Stereoselective binding of Human Serum Albumin. *Chirality* **2006**, *18*, 159−166.

(2) Brooks, W. H.; Daniel, K. G.; Sung, S.; Guida, W. C. Computational Validation of the Importance of Absolute Stereochemistry in Virtual Screening. *J. Chem. Inf. Model.* **2008**, *48*, 639−645.

(3) Escuder-Gilabert, L.; Martínez-Gómez, M. A.; Villanueva Camañas, R. M.; Sagrado, S.; Medina-Hernández, M. J. Microseparation techniques for the study of the enantioselectivity of drug-plasma protein binding. *Biomed. Chromatogr.* **2009**, *23*, 225−238.

(4) Varshney, A.; Sen, P.; Ahmad, E.; Rehan, M.; Subbaro, N.; Khan, R. H. Ligand binding Strategies of Human Serum Albumin: How can the cargo be utilised. *Chirality* **2010**, *22*, 77−87.

(5) Ghuman, J.; Zunszain, P. A.; Petitpas, I.; Bhattacharya, A. A.; Otagiri, M.; Curry, S. Structural Basis of the Drug-binding Specificity of Human Serum Albumin. *J. Mol. Biol.* **2005**, *353*, 38−52.
(6) Kragh-Hansen, U.; Chuang, V. T. G.; Otagiri, M. Practical Aspects of the Ligand-Binding and Enzymatic Properties of Human Serum Albumin. *Biol. Pharm. Bull.* **2002**, *25*, 695−704.
(7) Vuignier, K.; Schappler, J.; Veuthey, J. L.; Carrupt, P. A.; Martell, S. Drug-protein binding: a critical review of analytical tools. *Anal. Bioanal. Chem.* **2010**, *398*, 53−66.
(8) Asensi-Bernardi, L.; Martín-Biosca, Y.; Villanueva Camañas, R. M.; Medina-Hernández, M. J.; Sagrado, S. Evaluation of enantioselective binding of fluoxetine to human serum albumin by ultrafiltration and CE—Experimental design and quality considerations. *Electrophoresis* **2010**, *31*, 3268−3280.
(9) Sabela, M. I.; Gumede, N. J.; Escuder-Gilabert, L.; Martín-Biosca, Y.; Bisetty, K.; Medina-Hernández, M. J.; Sagrado, S. Connecting simulated, bioanalytical, and molecular docking data on the stereoselective binding of (±)-catechin to human serum albumin. *Anal. Bioanal. Chem.* **2012**, *402*, 1899−1909; Erratum. *Anal. Bioanal. Chem.* **2012**, *404*, 285.
(10) Zou, H. F.; Wang, H. L.; Zhang, Y. K. Stereoselective Binding of Warfarin and Ketoprofen to Human Serum Albumin Determined by Microdialysis Combined with HPLC. *J. Liq. Chromatogr. Relat. Techonol.* **1998**, *21*, 2663−2674.
(11) Miller, J. H. M.; Smail, G. A. Acute anti-inflammatory effects of aspirin and dexamethasone in rats deprived of endogenous prostaglandin precursors. *J. Pharm. Pharmacol.* **1977**, *29*, 235−237.
(12) O'Reilly, R. A. Interaction of Several Coumarin Compounds with Human and Canine Plasma Albumin. *J. Mol. Pharmacol.* **1971**, *7*, 209−218.
(13) Lagercrantz, C.; Larsson, T. Comparative studies of the binding of some ligands to human serum albumin non-covalently attached to immobilized Cibacron Blue, or covalently immobilized on Sepharose, by column affinity chromatography. *J. Biochem.* **1983**, *213*, 387−390.
(14) Wa, C.; Cerny, R. L.; Hage, D. S. Identification and quantitative studies of protein immobilization sites by stable isotope labeling and mass spectrometry. *Anal. Chem.* **2006**, *78*, 7967−7977.
(15) Huang, S. Y.; Zou, X. Advances and Challenges in Protein-Ligand Docking. *Int. J. Mol. Sci.* **2010**, *11*, 3016−3034.
(16) Mobley, D. L.; Dill, K. A. Binding of Small-Molecule Ligands to Proteins: "What you See" Is Not Always "What you Get. *Structure* **2009**, *17*, 489−498.
(17) Mohan, V.; Gibbs, A. C.; Cummings, M. D.; Jaeger, E. P.; DesJarlais, R. L. Docking: successes and challenges. *Curr. Pharm. Des.* **2005**, *11*, 323−333.
(18) Friesner, R. A.; Murphy, R. B.; Repasky, M. P.; Frye, L. L.; Greenwood, J. R.; Halgren, T. A.; Sanschagrin, P. C.; Mainz, D. T. Extra precision glide: docking and scoring incorporating a model of hydrophobic enclosure for protein-ligand complexes. *J. Med. Chem.* **2006**, *49*, 6177−6196.
(19) Deeb, O.; Rosales-Hernández, M. C.; Gómez-Castro, C.; Garduño-Juárez, R.; Correa-Basurto, J. Exploration of Human Serum Albumin Binding Sites by Docking and Molecular Dynamics Flexible Ligand−Protein Interactions. *Biopolymers* **2010**, *93*, 161−170.
(20) Sherman, W.; Day, T.; Jacobson, M. P.; Friesner, R. A.; Farid, R. Novel procedure for modeling ligand/receptor induced fit effects. *J. Med. Chem.* **2006**, *49*, 534−553.
(21) Rao, C. B.; Subramanian, J.; Sharma, S. D. Managing protein flexibility in docking and its applications. *Drug Discovery Today* **2009**, *14*, 394−400.
(22) Bos, O. J. M.; Fischer, M. J. E.; Wilting, J.; Janssen, L. H. M. Mechanism by which warfarin binds to human serum albumin. Stopped-flow kinetic experiments with two large fragments of albumin. *Biochem. Pharmacol.* **1989**, *38*, 1979−1984.
(23) QM-Polarized Ligand Docking protocol. *Schrödinger Suite 2011*; Schrödinger, LLC: New York, NY, 2011.
(24) Induced Fit Docking protocol. *Schrödinger Suite 2011*; Schrödinger, LLC: New York, NY, 2011.
(25) *Maestro*, version 9.2; Schrödinger, LLC: New York, NY, 2011.
(26) *Glide*, version 5.7; Schrödinger, LLC: New York, NY, 2011.
(27) *MacroModel*, version 9.9; Schrödinger, LLC: New York, NY, 2011.
(28) Protein Preparation Wizard. *Impact*, version 5.7; Schrödinger, LLC: New York, NY, 2011.
(29) *Prime*, version 3.0; Schrödinger, LLC: New York, NY, 2011.
(30) *Epik*, version 2.2; Schrödinger, LLC: New York, NY, 2011.
(31) *LigPrep*, version 2.5; *Epik*, version 2.2; Schrödinger, LLC: New York, NY, 2011.
(32) Cho, A. E.; Guallar, V.; Berne, B.; Friesner, R. A. Importance of Accurate Charges in Molecular Docking: Quantum Mechanical/Molecular Mechanical (QM/MM) Approach. *J. Comput. Chem.* **2005**, *26*, 915−931.
(33) Jaguar, version 7.8, Schrödinger, LLC, New York, NY, 2011.
(34) Li, W.; Liu, C.; Tan, G.; Zhang, X.; Zhu, Z.; Chai, Y. Molecular Modeling Study of Chiral Separation and Recognition Mechanism of β-Adrenergic Antagonists by Capillary Electrophoresis. *Int. J. Mol. Sci.* **2012**, *13*, 710−725.
(35) Jozwiak, K.; Moaddel, R.; Ravichandran, S.; Plazinska, A.; Kozak, J.; Patel, S.; Yamaguchi, R.; Wainer, I. W. Exploring enantiospecific ligand-protein interactions using cellular membrane affinity chromatography: Chiral recognition as a dynamic process. *J. Chromatogr., B* **2008**, *875*, 200−207.
(36) Lämmerhofer, M. Chiral recognition by enantioselective liquid chromatography: Mechanisms and modern chiral stationary phases. *J. Chromatogr., A* **2010**, *1217*, 814−856.
(37) Li, X.; Dash, R. K.; Pradham, R. K.; Qi, F.; Thompson, M.; Vinnakota, K. C.; Wu, F.; Yang, F.; Beard, D. A. A Database of Thermodynamic Quantities for the Reactions of Glycolysis and the Tricarboxylic Acid Cycle. *J. Phys. Chem. B* **2010**, *114*, 16068−16082.
(38) Alberty, R. A. Biochemical thermodynamics: applications of Mathematica. *Methods Biochem. Anal.* **2006**, *48*, 1−458.
(39) Alberty, R. A. Calculation of standard transformed Gibbs energies and standard transformed enthalpies of biochemical reactants. *Arch. Biochem. Biophys.* **1998**, *356*, 116−130.
(40) Koldsø, H.; Severinsen, K.; Tran, T. T.; Celik, L.; Jensen, H. H.; Wiborg, O.; Schiøtt, B.; Sinning, S. The two enantiomers of citalopram bind to the human serotonin transporter in reversed orientations. *J. Am. Chem. Soc.* **2010**, *132*, 1311−1322.
(41) Moroy, G.; Martiny, V. Y.; Vayer, P.; Villoutreix, B. O.; Miteva, M. A. Toward in silico structure-based ADMET prediction in drug discovery. *Drug Discovery Today* **2012**, *17*, 44−55.
(42) Shapira, M.; Abagyan, R.; Totrov, M. Nuclear Hormone Receptor Targeted Virtual Screening. *J. Med. Chem.* **2003**, *46*, 3045−3059.
(43) Davis, A. M.; Teague, S. J.; Kleywegt, G. J. Application and Limitations of X-ray Crystallographic Data in Structure-Based Ligand and Drug Design. *Angew. Chem., Int. Ed.* **2003**, *42*, 2718−2736.
(44) Kleywegt, G. J.; Henrick, K.; Dodson, E. J.; van Aalten, D. M. Pound-wise but penny-foolish: How well do micromolecules fare in macromolecular refinement? *Structure* **2003**, *11*, 1051−1059.
(45) Petitpas, I.; Bhattacharya, A. A.; Twine, S.; East, M.; Curry, S. Crystal Structure Analysis of Warfarin Binding to Human Serum Albumin. *J. Biol. Chem.* **2001**, *276*, 22804−22809.